Spectroelectrochemistry and Dimerization Equilibria of Chloro(terpyridine)platinum(II). Nature of the Reduced Complexes

Michael G. Hill,† James A. Bailey, Vincent M. Miskowski,* and Harry B. Gray*

Arthur Amos Noyes Laboratory, California Institute of Technology, Pasadena, California 91125

Received February 8, 1996[⊗]

$[Pt(tpy)Cl]^+$ (tpy is 2,2′:6′,2″-terpyridine) undergoes reversible one-electron reductions in 0.1 M TBAH/DMF (TBAH is tetrabutylammonium hexafluorophosphate) at $E°'_{+/0} = -0.74$ V and $E°'_{0/-} = -1.30$ V (*vs* AgCl (1.0 M KCl)/Ag). The first reduction couple is substantially positive of those observed for other M(II)−tpy complexes (for example, $E°'_{0/-} = -1.36$ V for $[Zn(tpy)Cl_2]$), a finding that suggests there is coupling between the empty $6p_z$ orbital of square planar Pt(II) and the π^* orbital of tpy, stabilizing the $(\pi^*)^1$ radical state. The dimerization constants of both $[Pt(tpy)Cl]^+$ and [Pt(tpy)Cl] in 0.1 M TBAH/DMF were determined spectroelectrochemically and found to be $8(1) \times 10$ and $10(4) \times 10\ M^{-1}$, respectively. On the basis of variable-concentration studies, a species observed at an intermediate level of reduction is formulated as the mixed-valence dimer $[(Pt(tpy)Cl)_2]^+$, with $K_{mix} = [(Pt(tpy)Cl)_2{}^+]/([Pt(tpy)Cl^+][Pt(tpy)Cl]) = 18(4) \times 10\ M^{-1}$. Analysis of variable-temperature EPR spectra indicates that the first reduction is ligand-centered ($^2B_2$) with substantial contributions from Pt(II) $5d_{yz}$ (4−6%) and $6p_z$ (3−4%). The second reduction is tentatively assigned as metal-centered; $5d_{x^2-y^2}$ is the likely acceptor orbital.

Introduction

Platinum(II) complexes of terpyridine have attracted considerable attention because of their interactions with biomolecules. They are known to intercalate into DNA[1,2] as well as bind to the histidine and arginine residues of proteins.[3,4] In addition, the chloro complex $[Pt(tpy)Cl]^+$ (tpy is 2,2′:6′,2″-terpyridine) interacts with itself; it oligomerizes in solution[1,5] and in the solid state,[1,2,5,6] and evidence for both ligand−ligand ($\pi-\pi$) and metal−metal interactions between monomers has been obtained.[5]

We are investigating the electronic structure of the Pt(tpy) unit (and related Pt(II) complexes of α-diimine ligands) as perturbed by various ancillary ligands and environments. Our work has shown that the energies of the lowest electronic transitions for a series of binuclear complexes (of the form $[(Pt(tpy))_2(\mu\text{-L})]^{n+}$) strongly correlate with the internuclear metal−metal distance.[7] In the course of photophysical studies of these complexes, we examined monomeric systems and encountered extremely complex behavior as a function of concentration and temperature.[5] Spectroelectrochemical experiments reported herein have shown that three different Pt(tpy) oxidation states form oligomers in DMF solution.

Experimental Section

Electrochemical experiments were performed using either a Bioanalytical Systems (BAS) Model 100 electrochemical analyzer or a Princeton Applied Research (PAR) Model 173 potentiostat controlled by a Model 175 universal programmer. Cyclic voltammetry (CV), chronocoulometry (CC), and Osteryoung square-wave voltammetry were performed at ambient temperature with a normal three-electrode configuration consisting of a platinum-disk working electrode and a AgCl/Ag reference electrode containing 1.0 M KCl. The working compartment of the electrochemical cell was separated from the reference compartment by a modified Luggin capillary. All three compartments contained a 0.1 M solution of supporting electrolyte. The dimethylformamide (Burdick and Jackson) was vacuum-distilled from KOH and CaO prior to use. TBAH (TBAH = tetrabutylammonium hexafluorophosphate) from Southwestern Analytical was used as received.

Reduction potentials are reported *vs* aqueous AgCl/Ag and are not corrected for the junction potential.[8] Under conditions identical with those employed here, the ferrocenium/ferrocene couple[9] has $E°' = 0.51$ V with $E_{pa} - E_{pc} = 94$ mV. No *iR* compensation was used.

UV−vis spectroelectrochemical experiments were carried out in an optically transparent thin-layer cell, consisting of vapor-deposited platinum working and pseudoreference electrodes and a platinum-wire auxiliary electrode.[10] The path length varied between 15 and 500 μm (depending on the particular experiment), and electrolysis times ranged between 2 and 20 s. Spectroscopic data were recorded on a Hewlett-Packard HP452 diode array spectrometer.

The compound $[Pt(tpy)Cl]Cl\cdot 2H_2O$ was prepared according to a standard method.[11] The PF_6^- salt of $[Pt(tpy)Cl]^+$ was prepared by metathesis with $[NH_4]PF_6$.[5] The PF_6^- salts of $[Pt(tpy)(NH_3)]^{2+}$ and $[Pt(tpy)(py)]^{2+}$ (py = pyridine) were prepared as yellow solids by the method reported[12] for the $B(C_6H_5)_4^-$ salt of $[Pt(tpy)(py)]^{2+}$, using $[NH_4]PF_6$ as the precipitant. The compound $[Zn(tpy)Cl_2]$[13] was prepared by mixing concentrated methanol solutions of $ZnCl_2$ and tpy in a stoichiometric ratio; the white solid that immediately precipitated was collected and air-dried.

† Present address: Department of Chemistry, Occidental College, Los Angeles, CA 90041.

⊗ Abstract published in *Advance ACS Abstracts,* July 1, 1996.

(1) Jennette, K. W.; Gill, J. T.; Sadownick, J. A.; Lippard, S. J. *J. Am. Chem. Soc.* **1976**, *98*, 6159.
(2) Jennette, K. W.; Lippard, S. J.; Vassiliades, G. A.; Bauer, W. R. *Proc Natl. Acad. Sci. U.S.A.* **1974**, *71*, 3839.
(3) Ratilla, E. M. A.; Scott, B. K.; Moxness, M. S.; Kostic, N. M. *Inorg. Chem.* **1990**, *29*, 918.
(4) Ratilla, E. M. A.; Kostic, N. M. *J. Am. Chem. Soc.* **1988**, *110*, 4427.
(5) Bailey, J. A.; Hill, M. G.; Marsh, R. E.; Miskowski, V. M.; Schaefer, W. P.; Gray, H. B. *Inorg. Chem.* **1995**, *34*, 4591.
(6) (a) Dewan, J. C.; Lippard, S. J.; Bauer, W. R. *J. Am. Chem. Soc.* **1980**, *102*, 858. (b) Constable, E. C.; Henney, R. P. G.; Leese, T. A.; Tocher, D. A. *J. Chem. Soc., Chem. Commun.* **1990**, 513. (c) Bailey, J. A.; Catalano, V. J.; Gray, H. B. *Acta Crystallogr.* **1993**, *C49*, 1598.
(7) Bailey, J. A.; Miskowski, V. M.; Gray, H. B. *Inorg. Chem.* **1993**, *32*, 369.
(8) Koepp, H. M.; Wendt, H.; Strehlow, H. Z. *Z. Elektrochem.* **1960**, *64*, 483.
(9) Gagne, R. R.; Koval, C. A.; Kisensky, G. C. *Inorg. Chem.* **1980**, *19*, 2854.
(10) Hill, M. G. Ph.D. Thesis, The University of Minnesota, 1992.
(11) (a) Morgan, G. T.; Burstall, F. H. *J. Chem. Soc.* **1934**, 1498. (b) Howe-Grant, M.; Lippard, S. J. *Inorg. Synth.* **1980**, *20*, 101.
(12) Basolo, F.; Gray, H. B.; Pearson, R. G. *J. Am. Chem. Soc.* **1960**, *82*, 4200.
(13) Douglas, J. E.; Wilkins, C. J. *Inorg. Chim. Acta* **1979**, *3*, 635.

S0020-1669(96)00137-1 CCC: $12.00

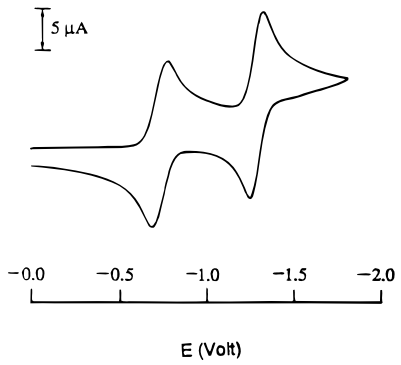

Figure 1. Cyclic voltammogram of 0.5 mM $[Pt(tpy)Cl]PF_6$ in 0.1 M TBAH/DMF. Scan rate = 100 mV/s.

Table 1. Electrochemical Data for Metal−py Complexes[a]

compound	1st redn	2nd redn	3rd redn
$[Pt(tpy)Cl]PF_6$	−0.74	−1.30	−2.1[b]
$[Pt(tpy)(NH_3)](PF_6)_2$	−0.63	−1.20	*c*
$[Pt(tpy)(py)](PF_6)_2$	−0.59	−1.08	−1.90
$[Zn(tpy)Cl_2]$	−1.36	*d*	*d*
$[Ru(tpy)_2](PF_6)_2$	−1.26	−1.50	*c*
$[Ru(bpy)_3](PF_6)_2$	−1.36	−1.54	−1.80
$[Pt(bpy)(py)_2](PF_6)_2$[e]	−0.88	−1.77	*c*

[a] Recorded in 0.1 M TBAH/DMF; V *vs* AgCl (1.0 M KCl)/Ag. Couples are reversible one-electron processes with $E_{pa} - E_{pc} = 80-90$ mV, except as noted. [b] Value at −20 °C. Irreversible at room temperature, with $E_{pc} = -2.2$ V. [c] Not measured. [d] Complicated irreversible reduction with cathodic maxima at about −1.8, −2.0, and −2.2 V. [e] Reference 18.

Results

Electrochemistry. Figure 1 shows the cyclic voltammogram of 1 mM $[Pt(tpy)Cl]PF_6$ in 0.1 M TBAH/DMF. Two chemically reversible reductions are observed ($E^{\circ\prime}_{+/0} = -0.74$ V and $E^{\circ\prime}_{0/-} = -1.30$ V), followed by an irreversible process at −2.2 V (*vs* AgCl/Ag). The irreversible reduction is quasi-reversible at −20 °C, with $E^{\circ\prime}_{-/2-} = -2.1$ V; it is likely coupled to loss of Cl^- from the triply reduced complex, as all three reductions are reversible at room temperature for $[Pt(tpy)(py)]^{2+}$ (Table 1). Bulk electrolysis and chronocoulometry confirm that each reduction corresponds to one electron per platinum center. Qualitatively, this electrochemical response is similar to those of other metal ion−α-diimine complexes, which generally undergo sequential $1e^-$ ligand-based reductions. For $[Pt(tpy)Cl]^+$, however, $E^{\circ\prime}_{+/0}$ and $E^{\circ\prime}_{0/-}$ are at unusually positive potentials. For example, the first reduction of $[Zn(tpy)Cl_2]$ occurs at −1.36 V, while those of $[Ru(tpy)_2]^{2+}$ and $[Os(tpy)_2]^{2+}$ are reported at −1.15 and −1.09 V (*vs* AgCl/Ag), respectively.[14] Interestingly, a similar trend has been observed for the reductions of analogous $Pt(bpy)X_2$ (bpy is 2,2'-bipyridine) compounds (Table 1). This latter effect has been attributed to mixing of α-diimine π^* orbitals with the Pt(II) metal orbitals;[15] our finding that the shift is somewhat larger for $[Pt(tpy)Cl]^+$ led to additional study.

Spectroelectrochemistry. In principle, the positive shift in the reduction potentials of $[Pt(tpy)Cl]^+$ could originate from oligomerization reactions that stabilize the reduced products relative to monomeric [Pt(tpy)Cl]. In order to investigate this possibility, we carried out spectroelectrochemical experiments designed to identify any oligomeric materials. Figure 2 shows the UV−vis spectroelectrochemical reduction of 1 mM $[Pt(tpy)Cl]PF_6$ in 0.1 M TBAP/DMF. As the potential is swept past the first wave, the initial bands at 285, 335, 352, and 380−400 nm disappear, while new absorbances at 366, 409, 504 (sh), 543, and 770 nm grow in. A very similar (but red-shifted) spectrum is obtained after the first reduction of $[Zn(tpy)Cl_2]$, with bands growing in at 372, 405, 435 (sh), 560 (sh), 600, and >800 nm. Electrolysis of $[Pt(tpy)Cl]^+$ past the second wave produces a species with absorbances at 310, 330 (sh), 395, 460, and >800 nm. Each of these processes is reversible on the spectroelectrochemical time scale, as evidenced by the quantitative regeneration of the initial spectrum upon reoxidation.

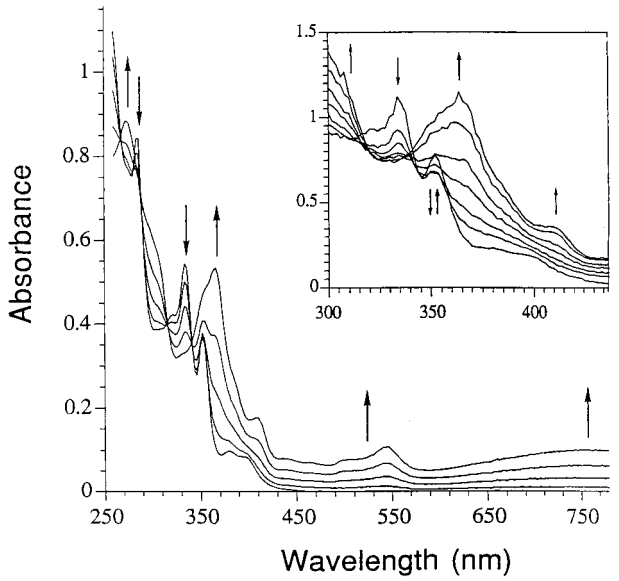

Figure 2. Spectroelectrochemistry of the first reduction process of 1.0 mM $[Pt(tpy)Cl]PF_6$ in 0.1 M TBAH/DMF. Inset: spectroelectrochemical reduction of 12.0 mM $[Pt(tpy)Cl]PF_6$ in 0.1 M TBAH/DMF.

Examination of $[Pt(tpy)Cl]^{n+}$ spectral changes revealed several features that can only be explained by invoking the existence of multiple equilibrium reactions. For example, despite the apparent isosbestic behavior shown in Figure 2, plots of the normalized change in absorbance at several different wavelengths *vs* the percent completion of electrolysis reveal the existence of a second reduced product at early stages of the electrolysis. The relative concentration of this species increases with higher initial concentrations of $[Pt(tpy)Cl]^+$, such that, at total platinum concentrations greater than ∼5 mM, a distinctly nonisosbestic spectroelectrochemical response is observed (Figure 2, inset). On the basis of this and several other observations (*vide infra*), we formulate this intermediate species as a [Pt(tpy)Cl]−$[Pt(tpy)Cl]^+$ ($[(Pt(tpy)Cl)_2]^+$) mixed-valence dimer.

Solutions of both $[Pt(tpy)Cl]^+$ and [Pt(tpy)Cl] exhibit non-Beers-law behavior at concentrations above ∼0.1 mM in 0.1 M TBAP/DMF. Plots[1] of $((\epsilon_m - \epsilon)/[Pt_{total}])^{1/2}$ *vs* $(\epsilon_m - \epsilon)$ (where ϵ_m is the monomer extinction coefficient (infinite dilution) and ϵ is the apparent extinction coefficient) yield straight lines for each complex (Figure 3). From these data, we calculate a value of $8(1) \times 10\ M^{-1}$ for the dimerization constant of $[Pt(tpy)Cl]^+$ (K_{ox}) and a value of $10(4) \times 10\ M^{-1}$ for the dimerization constant of [Pt(tpy)Cl] (K_{red}). The value for K_{ox} in 0.1 M TBAH/DMF is small relative to that in 0.1 M NaCl/water ($K_{ox} = 4(2) \times 10^3\ M^{-1}$).[1] The lower dielectric constant of DMF disfavors the formation of a dicationic dimer. Because of the combination of the small magnitude of K_{ox} and the limited solubility of available $[Pt(tpy)Cl]^+$ salts in DMF, we were unable to obtain sufficiently high dimer concentrations to directly observe a visible absorption band attributable to a $[(Pt(tpy)Cl)_2]^{2+}$ metal−metal-bonded dimer.[5]

(14) Berger, R. M.; McMillin, D. R. *Inorg. Chem.* **1988**, *27*, 4245.
(15) (a) Collison, D.; Mabbs, F. E.; McImnes, E. J. L.; Taylor, K. J.; Welch, A. J.; Yellowlees, L. J. *J. Chem. Soc., Dalton Trans.* **1996**, 329. (b) Klein, A.; Kaim, W. *Organometallics* **1995**, *14*, 1176.

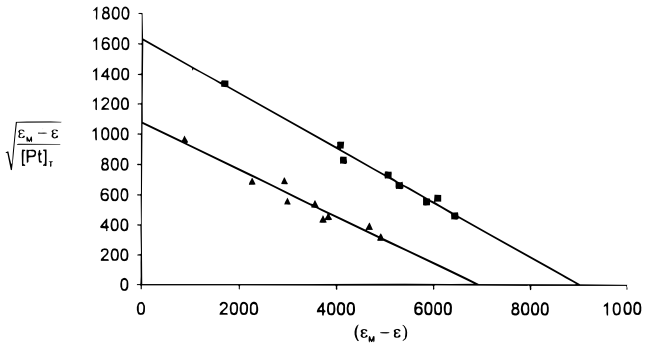

Figure 3. Dimerization plots for [Pt(tpy)Cl]PF_6 in 0.1 M TBAH/DMF (▲) and electrochemically generated [Pt(tpy)Cl] in 0.1 M TBAH/DMF (■).

Scheme 1

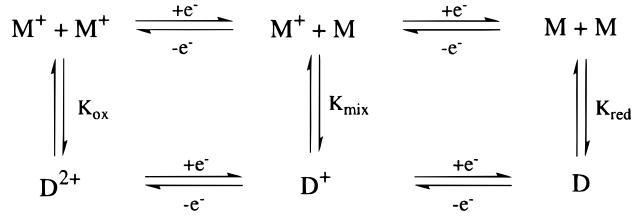

Given K_{ox}, K_{red}, $\epsilon([Pt(tpy)Cl]^+)$, and $\epsilon([Pt(tpy)Cl])$, values for $\epsilon([(Pt(tpy)Cl)_2]^{2+})$ and $\epsilon([(Pt(tpy)Cl)_2])$ could be calculated at any wavelength. We were able to fit the resulting spectral changes for the spectroelectrochemical reduction according to Scheme 1,[16] by assuming an equilibrium constant for the formation of $[(Pt(tpy)Cl)_2]^+$ (K_{mix}) equal to 18(4) × 10 M^{-1}. At 353 nm, the absorbance initially decreases, minimizes approximately one-third of the way through the electrolysis, and then increases to a maximum value at 1e^-/mol added. At each point along the electrolysis, there is good agreement between the experimental data and our fit. To check the internal consistency of our analysis, we plotted the observed percent electrolysis *vs* the calculated percent electrolysis (based on the concentrations of $[Pt(tpy)Cl]^+$, $[(Pt(tpy)Cl)_2]^{2+}$, and $[(Pt(tpy)Cl)_2]^+$ determined from the absorbance at 353 nm and our values of K_{ox}, K_{red}, K_{mix}, $\epsilon([Pt(tpy)Cl]^+)$, $\epsilon([Pt(tpy)Cl])$, $\epsilon([(Pt(tpy)Cl)_2]^{2+})$, $\epsilon([(Pt(tpy)Cl)_2])$, and $\epsilon([(Pt(tpy)Cl)_2]^+)$) and obtained a straight line with slope equal to 1. Spectra for the various monomeric and dimeric species were calculated from the data with our parameters and are shown in Figure 4. The spectrum of $[(Pt(tpy)Cl)_2]^+$ is not shown, as it was only well-determined near 350 nm (showing a decrease in absorption in this region relative to other species); the computed spectrum in other spectral regions is extremely noisy, and no well-defined maxima are evident.

EPR Spectroscopy. The EPR spectra of electrochemically reduced solutions of $[Pt(tpy)Cl]^+$ are in qualitative agreement with this model. Fluid solutions of [Pt(tpy)Cl] (∼0.1 mM in 0.1 M TBAH/DMF) exhibit a temperature-dependent isotropic signal at $g = 1.98$ with no resolved hyperfine splitting.[17] Lowering the temperature causes a steady decrease in the doubly integrated signal intensity, consistent with the formation of a diamagnetic $[(Pt(tpy)Cl)_2]$ dimer. Frozen at 77 K, this same solution shows a rhombic signal (Figure 5) with $g_1 = 2.014$, $g_2 = 2.006$, $g_3 = 1.913$ and $|A_1|(^{195}Pt) = 70 \times 10^{-4}$, $|A_2|(^{195}Pt) = 48 \times 10^{-4}$ cm^{-1}. We were unable to resolve the platinum hyperfine splitting of g_3; however, computer simulations establish an upper limit based upon the experimental line width and the absence of resolved splitting: $|A_3|(^{195}Pt) \leq 18 \times 10^{-4}$ cm^{-1}. These spectra, which are very similar to the reported fluid and frozen solution spectra of $[Pt(bpy)Cl_2]^-$ and [Pt(bpy)-

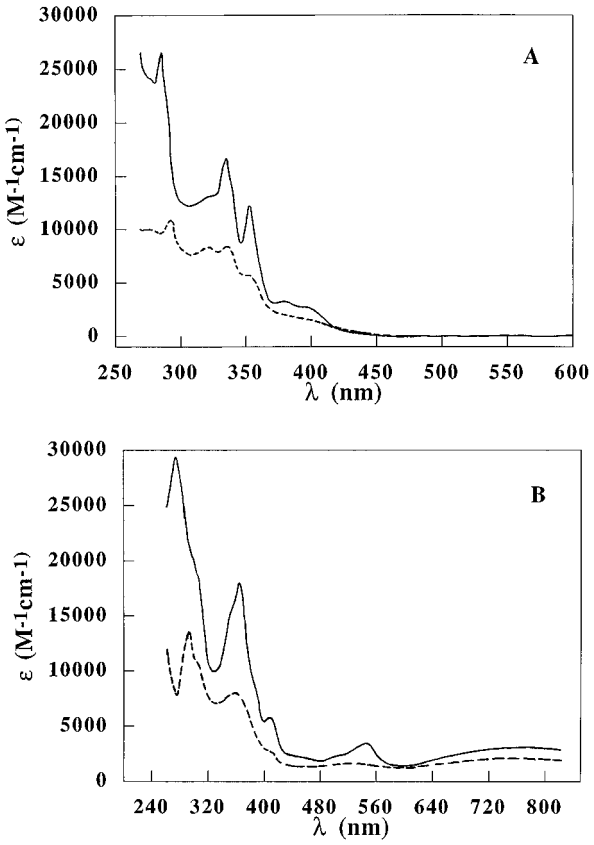

Figure 4. Calculated electronic spectra in 0.1 M TBAH/DMF: A, $[Pt(tpy)Cl]^+$ (—) and $[(Pt(tpy)Cl)_2]^{2+}$ (- - -); B, [Pt(tpy)Cl] (—) and $[(Pt(tpy)Cl)_2]$ (- - -). The extinction coefficients in these figures are defined per Pt.

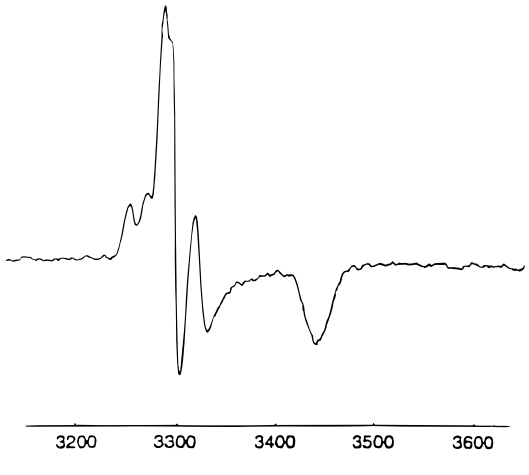

Figure 5. X-Band EPR spectrum of [Pt(tpy)Cl] (0.1 mM) in frozen 0.1 M TBAH/DMF at 77 K.

(16) The data at 353 nm were fit by an iterative numerical method that simultaneously minimized the sum of differences of squares between the measured and calculated (a) absorbances and (b) electron equivalents added, together with mass balance used as a constraint. Values used for fit: $K_{ox} = 8(1) \times 10$ M^{-1}; $K_{red} = 10(4) \times 10$ M^{-1}; $\epsilon([Pt(tpy)Cl]^+) = 12\,200$ M^{-1} cm^{-1}; $\epsilon([Pt(tpy)Cl]) = 14\,900$ M^{-1} cm^{-1}; $\epsilon([(Pt(tpy)Cl)_2]^{2+}) = 10\,600$ M^{-1} cm^{-1}; $\epsilon([(Pt(tpy)Cl)_2]) = 15\,000$ M^{-1} cm^{-1}. The best-fit values of the two variable parameters are $K_{mix} = 18(3) \times 10$ M^{-1} and $\epsilon([(Pt(tpy)Cl)_2]^+) = 2000$ M^{-1} cm^{-1}. We note that this approach is best suited to a wavelength that has $\epsilon([(Pt(tpy)Cl)_2]^+)$ very different from the other ϵ's. For our data sets, this condition was only well-satisfied over the small range of $\lambda \cong$ 350−355 nm.

$(L)_2]^+$ (L = pyridine or ammonia) complexes,[15,18] confirm that the first reduction is essentially ligand-based. Specifically, the sign of the anisotropic splitting ($g_1 \approx g_2 \approx g_e \gg g_3$) recorded at 77 K is inconsistent with that expected for a planar Pt(I) ($x^2 - y^2$)^1 ground state.[19]

Addition of a large excess of $[Pt(tpy)Cl]^+$ to the radical species described above has little effect on the *g* value for fluid solutions,[17] but frozen solutions so prepared exhibit an unstructured, isotropic signal with *g* similar to the room-temperature value. The spectroelectrochemical results suggest that equilibrium mixtures of dimers and monomers are formed. The mixed-valence dimer is entropically favored relative to [Pt(tpy)Cl] at low temperature and is presumably responsible for the unstructured EPR signal of the frozen solutions. Electron exchange between the halves of the mixed-valence dimer may explain the lack of hyperfine structure.

Discussion

We have found that $[Pt(tpy)Cl]^+$ and its one-electron reduction product [Pt(tpy)Cl] form both homo- and mixed-valence dimers in 0.1 M TBAH/DMF. Solution dimerization of $[Pt(tpy)Cl]^+$ in water has been analyzed previously,[1,5] and it is reasonable that the reduced (less highly charged) dimers should also be stable. There is crystallographic evidence both for metal−metal and ligand−ligand ($\pi-\pi$) bonding interactions in the solid-state oligomers of Pt(II) α-diimine complexes,[1,5,6] and there is spectroscopic evidence for both types of oligomer interactions in solution and in the solid state.[5,7,20]

The major consequence of dimerization on the electronic spectra of the dimers is that the absorption bands of the monomers (which are primarily tpy-localized transitions, π-to-π^* or, for the radicals, π^*-to-π^*)[21] are broadened (Figure 4). This is consistent with ligand−ligand $\pi-\pi$ interactions in the dimers;[22] however, we cannot exclude significant Pt−Pt interactions because metal−metal transitions are probably too weak[5,7] to be observed for these complexes.

The large anodic shift in the reduction potentials of $[Pt(tpy)Cl]^+$ relative to other M(II)−tpy compounds cannot be accounted for solely on the basis of the difference between the dimerization constants of $[Pt(tpy)Cl]^+$ and [Pt(tpy)Cl] ($(RT/F)\ln(K_{ox}/K_{red}) \approx -0.03$ V), so another explanation must be sought. It has long been known that interaction between the empty $(n+1)p_z$ orbital of d^8 square planar complexes with the empty π^* orbitals of π-back-bonding ligands results in a substantial stabilization of the lower energy of the two orbitals.[23] Note that the $(n+1)p_z$ metal orbital plays a special role in square planar stereochemistry: it is strongly destabilized for pseudooctahedral complexes (such as $[Ru(tpy)_2]^{2+}$) by σ-symmetry metal−ligand interactions and is therefore less available for π-symmetry interactions with the ligands. We suggest (as have others for Pt(II) α-diimine complexes)[15,18] that mixing of π^*-(tpy) orbitals with $6p_z$(Pt) is responsible for the relative ease of reduction of $[Pt(tpy)Cl]^+$.

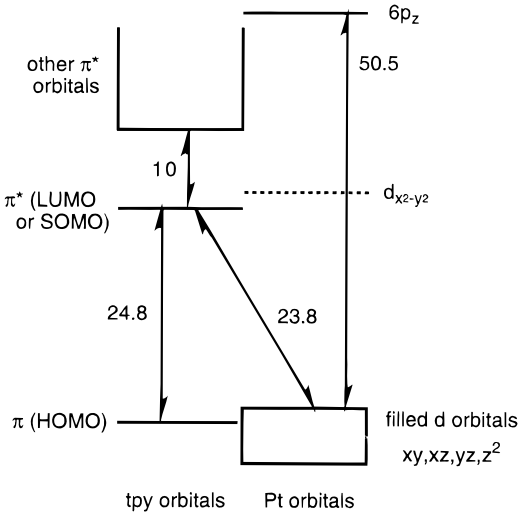

Figure 6. Molecular orbital diagram for a Pt(II) complex of tpy or tpy$^-$. Energy differences ($\times 10^3$, cm^{-1}) are estimated as indicated in the text.

The energies of the various states are summarized in Figure 6. The lowest-energy singlet−singlet and singlet−triplet $\pi \rightarrow \pi^*$ tpy excitations of $[Pt(tpy)Cl]^+$ have been located at 28 400 and 21 300 cm^{-1}.[5] The lowest-energy ^{1}MLCT ($d \rightarrow \pi^*$(tpy)) excited state lies at 25 600 cm^{-1}, and the singlet−triplet splitting can be estimated (by comparison to related α-diimine complexes) to be ~3500 cm^{-1}.[20c] This places ^{3}MLCT at 22 100 cm^{-1}, just barely above $^3(\pi \rightarrow \pi^*)$. Experimentally, the dilute monomer emission at 77 K is unequivocally from the $^3(\pi \rightarrow \pi^*)$ state.[5] The one-electron π/π^* and $d\pi/\pi^*$ splittings are roughly estimated as the average of the singlet−singlet and singlet−triplet excitation energies in Figure 6, which makes them virtually identical. Aldridge *et al.*[24] have assigned the luminescence of dilute $[Pt(tpy)X]^+$ (X = NCS, OH, OCH_3) to ^{3}MLCT states, emphasizing the delicate energetic balance of these states. The energy of the empty $d_{x^2-y^2}$ level is not spectroscopically established for $[Pt(tpy)Cl]^+$, but it cannot lie much above the lowest π^*(tpy) level because a ^{3}(dd) state is the lowest-energy excited state of $[Pt(bpy)Cl_2]$.[20c]

The visible absorption bands of the metal-bound tpy anion radical are assigned to transitions from the SOMO (singly occupied molecular orbital) to higher-energy π^* levels, by analogy to the well-studied (and very similar) bpy anion radical spectrum.[21] The lowest-energy band (Figure 2) places the next-highest π^* level about 10 000 cm^{-1} above the SOMO for [Pt(tpy)Cl] and a few thousand reciprocal centimeters lower than that for $[Zn(tpy)Cl_2]^-$. An estimate of the "zero-order" magnitude of the splitting of the filled d orbitals and $6p_z$ is available from the assigned $^1(d_{z^2} \rightarrow p_z)$ transition of $[Pt(NH_3)_4]^{2+}$, which occurs at 51 200 cm^{-1}.[25] This value suggests that the $6p_z$(Pt) level lies about 25 000 cm^{-1} (3 eV) above the lowest-energy π^*(tpy) level. We have assumed a singlet−triplet $d_{z^2} \rightarrow p_z$ splitting of 3500 cm^{-1} for the one-electron $d_{z^2} \rightarrow p_z$ spacing (the average of singlet−singlet and singlet−triplet energies)[26] included in Figure 6.

(17) Our first measurement of the room-temperature EPR spectrum showed resolved hyperfine splitting and was very similar to the spectrum of $Pt(bpy)Cl_2^-$.[15a] Unfortunately, we have been unable to reproduce this result, despite many attempts. Contamination of our samples with small amounts of $[Pt(tpy)Cl]^+$ may conceivably result in exchange broadening in fluid solution.

(18) (a) Braterman, P. S.; Song, J.-I.; Wimmer, F. M.; Wimmer, S.; Kaim, W.; Klein, A.; Peacock, R. D. *Inorg. Chem.* **1992**, *31*, 5084. (b) Braterman, P. S.; Song, J.-I.; Vogler, C.; Kaim, W. *Inorg. Chem.* **1992**, *31*, 222.
(19) McGarvey, B. R. In *Transition Metal Chemistry*; Carlin, R. L., Ed.; Marcel Dekker: New York, 1967; Vol. 3, p 89.
(20) (a) Miskowski, V. M.; Houlding, V. H. *Inorg. Chem.* **1989**, *28*, 1529. (b) Houlding, V. H.; Miskowski, V. M. *Coord. Chem. Rev.* **1991**, *111*, 145. (c) Miskowski, V. M.; Houlding, V. H.; Che, C.-M.; Wang, Y. *Inorg. Chem.* **1993**, *32*, 2518.
(21) König, E.; Kremer, S. *Chem. Phys. Lett.* **1970**, *5*, 87.
(22) (a) Birks, J. B. *Photophysics of Aromatic Molecules*; Wiley-Interscience: New York, 1970. (b) Birks, J. B.; Dyson, D. J.; Munro, I. H. *Proc. R. Soc. A* **1963**, *275*, 575.
(23) Gray, H. B.; Ballhausen, C. J. *J. Am. Chem. Soc.* **1963**, *85*, 260.
(24) Aldridge, T. K.; Stacey, E. M.; McMillin, D. R. *Inorg. Chem.* **1994**, *33*, 722.
(25) Anex, B. G.; Takeuchi, N. *J. Am. Chem. Soc.* **1974**, *96*, 4411.
(26) Rice, S. F.; Gray, H. B. *J. Am. Chem. Soc.* **1983**, *105*, 4571.

Defining the molecular axes as shown below, the tpy π and π^* orbitals are of A_2 and B_2 symmetries (the C_{2v} rotation axis is the y axis) and can therefore bond with d_{xz} and d_{yz} metal orbitals, respectively. The B_2 orbitals can additionally interact with the empty $6p_z$(Pt).

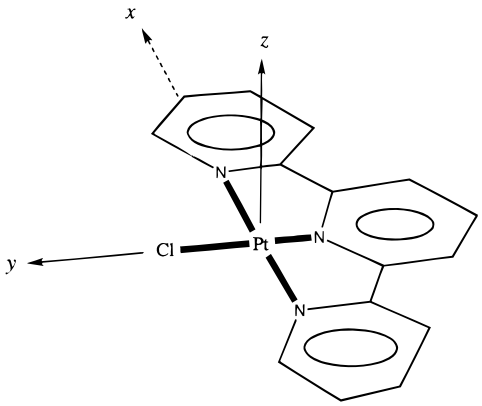

For metal-bound bpy ligands, the LUMO has B_2 symmetry,[21,27] with the next lowest-energy π^* level (7000 cm^{-1} higher in energy) A_2; the bpy HOMO is also A_2. While the frontier orbital symmetries are not established for tpy, the spectral similarity of singly reduced Pt(II) complexes of bpy[15a,18] and tpy strongly suggests similar symmetries.

For the Zn(II) complex, significant mixing of the metal orbitals with the π and π^* orbitals of the bound tpy ligand can be excluded on energetic grounds; the occupied 3d metal orbitals are too stable, while the empty metal 4p orbitals lie at inaccessibly high energy.[28] Interaction with the filled d_{xz} or d_{yz} orbital must destabilize the LUMO. The considerable *stabilization* of the LUMO of $[Pt(tpy)Cl]^+$ relative to $[Zn(tpy)Cl_2]$ indicated by the 0.62 V (~5000 cm^{-1}) anodic shift of the first reduction therefore suggests significant π^*-(LUMO)−$6p_z$(Pt) mixing for the Pt(II) complex. Note that this is consistent with the blue shift observed for the lowest-energy $\pi^* \rightarrow \pi^*$ transition of [Pt(tpy)Cl] relative to $[Zn(tpy)Cl_2]^-$ (assuming that the SOMO is B_2, and the second-lowest energy π^* level is A_2).

Analysis of the EPR spectrum yields further insight into the bonding. With the empty $d\sigma^*$ $d_{x^2-y^2}$ orbital being A_1, the spin−orbit operator H_{SO} can mix $d_{x^2-y^2}$ into the π^* SOMO of [Pt(tpy)Cl] via $\mathbf{L}_y$ and $\mathbf{L}_x$ to affect g_y and g_x for the $^2A_2$ and $^2B_2$ radical states, respectively. The simple result[19] for the unique g value (designated $g_{\|}$) is

$$g_{\|} = g_e - \frac{2\xi\rho_d}{E(x^2-y^2) - E(\pi^*)} \qquad (1)$$

Here ξ is the 5d(Pt) spin−orbit coupling constant, ~3500 cm^{-1}, and ρ_d is the 5d(Pt) contribution (xz or yz) to the SOMO (the $x^2 - y^2$ level is assumed to be pure d).[29] Note that ρ_d is the square of the MO coefficient, hence positive-definite. The observed Δg_3 (*i.e.*, $g_3 - g_e$) is −0.089. Braterman *et al.*[18] have pointed out that the *second* reduction of Pt(II)−α-diimine complexes is largely metal-centered because the electronic absorption spectra of the doubly reduced complexes are similar to those of the singly reduced complexes, whereas the spectrum of doubly reduced free bpy is strongly shifted from that of singly reduced bpy.[21] Our observations for $[Pt(tpy)Cl]^+$ are consistent in this regard, and the difference between the first and second reduction potentials (0.56 V), when corrected for coupling effects (which should be largely electrostatic in nature, as the $d_{x^2-y^2}$ and π^* levels are only weakly electronically coupled), may then provide a measure of $E(x^2 - y^2) - E(\pi^*)$ (ΔE). Using the difference between the first two reduction potentials of $[Ru(bpy)_3]^{2+}$ (0.18 V) as the correction, we estimate a value for ΔE of 0.38 eV (3070 cm^{-1}); eq 1 then yields $\rho_d = 0.04$. If we instead interpret the *third* reduction of $[Pt(tpy)Cl]^+$ (at −2.1 V) as the metal-centered process, the corrected ΔE is 9520 cm^{-1} and the calculated ρ_d increases to 0.12. The first calculation seems more reasonable; but, in either case, there is significant mixing of $d_{xz}(d_{yz})$ into the SOMO.

Two additional effects on the g values can be envisioned. First, the filled d levels can mix with the xz or yz component of the SOMO *via* H_{SO}. Including these terms, we obtain the following expressions for the g values of a $^2B_2$ radical state:

$$g_{\|} = g_x = g_e - \frac{2\xi\rho_d}{E(x^2-y^2) - E(\pi^*)} + \frac{6\xi\rho_d}{E(\pi^*) - E(z^2)} \qquad (2)$$

$$g_y = g_e + \frac{2\xi\rho_d}{E(\pi^*) - E(xy)} \qquad (3)$$

$$g_z = g_e + \frac{2\xi\rho_d}{E(\pi^*) - E(xz)} \qquad (4)$$

The additional terms in eqs 3 and 4 are probably responsible for the positive values of Δg_1 and Δg_2, but these are very small because $\Delta E \geq 24\,000$ cm^{-1} (Figure 6). Inclusion of the correction term for g_x (eq 2) with this rough estimate for $E(\pi^*) - E(z^2)$ (24 000 cm^{-1}) increases the calculated ρ_d to 0.06. However, $E(\pi^*) - E(z^2)$ is likely to be considerably larger than the estimate,[30] so the calculation of ρ_d without this term is preferred.

Second, a $^2B_2$ state may have $6p_z$(Pt) character, and H_{SO} can additionally affect the g values by mixing the $6p_z$(Pt) component of the SOMO with $6p_{x,y}$(Pt) levels. However, values for $E(p_{x,y}) - E(\pi^*)$ are very large (presumably much larger than $E(p_z) - E(\pi^*)$, which is ~25 000 cm^{-1}), so these terms can be ignored. Consequently, the g values give no information as to the $6p_z$-(Pt) content of the SOMO. However, the hyperfine coupling terms do. Assuming a $^2B_2$ state, we have[19,31]

$$A_{\|} = A_x = \langle A\rangle + P[(\Delta g_x) - {}^4/_7\rho_d - {}^2/_5\rho_p] \qquad (5)$$

$$A_y = \langle A\rangle + P[(\Delta g_y) + {}^2/_7\rho_d - {}^2/_5\rho_p] \qquad (6)$$

$$A_z = \langle A\rangle + P[(\Delta g_z) + {}^2/_7\rho_d + {}^4/_5\rho_p] \qquad (7)$$

P is the dipolar coupling parameter, equal to 492×10^{-4} cm^{-1} for platinum;[31] $\langle A\rangle$ is the isotropic coupling, and ρ_p refers to $6p_z$(Pt). Since the g values are nearly axial, the large rhombic character of the observed platinum hyperfine coupling *must* reflect ρ_p, which confirms a $^2B_2$ assignment for the singly reduced state. We cannot fully analyze eqs 5−7 because we

(27) Kober, E. M.; Meyer, T. J. *Inorg. Chem.* **1984**, *23*, 3877.
(28) Ballhausen, C. J.; Gray, H. B. *Molecular Orbital Theory*; W. A. Benjamin, Inc.: New York, 1965.
(29) The $x^2 - y^2$ level is actually likely to be only 60−80% d, in which case the calculated ρ_d is increased by a factor of 1.2−1.8.
(30) The experimental energy ordering of the filled d orbitals of tetragonal Pt(II) complexes is $xy > xz,yz > z^2$ (Martin, D. S., Jr. *Inorg. Chim. Acta* **1971**, *5*, 107). For example, the singlet−singlet transitions of $[PtCl_4]^{2-}$ have been assigned at 26 050 ($xy \rightarrow x^2 - y^2$), 29 575 ($xz,yz \rightarrow x^2 - y^2$), and 36 500 cm^{-1} ($z^2 \rightarrow x^2 - y^2$). The value of $E(\pi^*) - E(z^2) = 24\,000$ cm^{-1} used in the calculation of ρ_d is likely to be too small; hence ρ_d will be too large.
(31) Morton, J. R.; Preston, K. F. *J. Magn. Reson.* **1977**, *30*, 577.

have only an upper limit for $|A_3|$ and lack a measurement of $|A_{iso}|$. However, reported values[18a,32] of $|A_{iso}| = 34 \times 10^{-4}$ cm^{-1} for $[Pt(bpy)(py)_2]^+$ and 54×10^{-4} cm^{-1} for $[Pt(bpy)Cl_2]^-$ are consistent with A_1 and A_2 having the same sign for these radicals, and we assume this to be true for [Pt(tpy)Cl] as well. Interpreting A_1 and A_2 as A_y and A_z, we calculate (from the difference of eqs 6 and 7) that $\rho_p = 0.044$ or 0.031, depending on whether A_1 is A_y or A_z.[33] Our values for ρ_p and ρ_d are slightly larger than those recently calculated (using an extended Huckel method) for the SOMO of $[Pt(bpy)Cl_2]^-$.[15a]

Given the apparent stabilization of the π^* orbitals as indicated above, a ~5300 cm^{-1} red shift of the energies of the $\pi-\pi^*$ transitions might be expected for a Pt(II)−α-diimine complex relative to other M(II)−α-diimine species; however, a comparison of the energies of the lowest $^1(\pi \rightarrow \pi^*)$ transitions of $[Pt(tpy)Cl]^+$ (28 400 cm^{-1}) and $[Zn(tpy)Cl_2]$ (29 900 cm^{-1}) reveals a shift of only 1500 cm^{-1}. Evidently, the stabilization of the ligand π^* LUMO of $[Pt(tpy)Cl]^+$ must be largely offset by a compensatory stabilization of the ligand π HOMO through coupling with the filled $d_{xz,yz}$ Pt(II) orbitals. It should be noted that, depending on the energy of the $d_{xz,yz}$ orbitals, the ligand π orbitals could be either stabilized or destabilized by this coupling. While the Pt(III)/Pt(II) and tpy^+/tpy redox couples are unknown for $Pt(tpy)Cl^+$,[34] the similar energies of the Pt(II) monomer MLCT ($d \rightarrow \pi^*$) and $\pi \rightarrow \pi^*$ electronic transitions[5,20c] are consistent with similar energies for the occupied π(tpy) and 5d(Pt) orbitals (Figure 6).

Finally, we note that the $p_z-\pi^*$ interaction seems to be somewhat more important for Pt(II)−tpy complexes than for Pt(II)−bpy analogues. For example, the difference in reduction potentials between $[Pt(bpy)(py)_2]^{2+}$ and $[Ru(bpy)_3]^{2+}$ is 425 mV, while that between $[Pt(tpy)py]^{2+}$ and $[Ru(tpy)_2]^{2+}$ is 550 mV (Table 1). The central Pt−N bond of the terpyridine complexes is significantly shorter (~0.1 Å) than the other two Pt−N distances, owing to a ligand-imposed geometric constraint;[5,35] it follows, therefore, that the overall $p_z-\pi^*$ mixing should be more extensive in tpy than in bpy complexes.

Acknowledgment. J.A.B. acknowledges an NSERC (Canada) Postdoctoral Fellowship. This work was supported by the National Science Foundation.

IC960137J

(32) Klingler, R. J.; Huffman, J. C.; Kochi, J. K. *J. Am. Chem. Soc.* **1982**, *104*, 2147.

(33) These two solutions for ρ_p require that A_1 and A_2 be either both positive ($\rho_p = 0.044$) or both negative ($\rho_p = 0.031$).

(34) A reversible Pt(III)/Pt(II) couple has been observed for Pt(bpy)(mesitylene)$_2$ and several other sterically blocked Pt(II) square planar complexes (see ref 15b and references therein).

(35) (a) Hecker, C. R.; Fanwick, P. E.; McMillin, D. R. *Inorg. Chem.* **1991**, *30*, 659. (b) Leising, R. A.; Kubow, S. A.; Churchill, M. R.; Buttren, L. A.; Ziller, J. W.; Takeuchi, K. J. *Inorg. Chem.* **1990**, *29*, 1306.